European Journal of Molecular & Clinical Medicine
ISSN 2515-8260 Volume 07, Issue 07, 2020

Magnetic Properties Of Bismuth Substituted Strontium Ferrite Nanoparticles

Deepak Basandrai[1]

[1]*Department of Physics, School of Physical Sciences and Chemical Engineering, Lovely Professional University, Phagwara, Punjab 144411, India*

[1]*deepakbasandrai@gmail.com*

ABSTRACT: The Y-type hexaferrites $Sr_2CO_{2-X}Bi_xFe_{12}O_{22}$ (x=0.0, 0.05 and 0.10) has been synthesized using Sol Gel technique. The structural and magnetic outcome of Bismuth dopant was investigated by XRD, FTIR and VSM study. The XRD reveal the formation of Y-type hexaferrite. Two prominent peaks were observed near 400-600 cm^{-1} in FTIR spectra indicates twisting and broadening of Fe-O bond at octahedral and tetrahedral sites, respectively. The squareness ratio (M_r/ M_s) of less than 0.5 for all compositions reveals that nanoparticles are haphazardly oriented multi domain particles.

Key Words: Y-type hexaferrites, Sol Gel auto Combustion method, XRD, FTIR, VSM

1.Introduction:

Hexaferrites have a wide range property which runs from having high resistivity to having good dielectric properties and much more [1-4]. Hexaferrites become important by virtue of their unmatchable magnetic and mechanical parameters. The understanding of these materials has led to wide range research and technological advancement. Today Hexaferrites found their extensive use in electronic industry. Due to their high permeability and high temperature stability they are used in filter circuits, transformers using high frequency and other circuits [5]. The excellent magnetic behaviors make them capable of modern-day applications such as ferrite cores, ferrite magnets and their uses in microwave devices. They are also known to have applications in non-volatile memory of computers which are made up of ferrites [6]. Hexaferrite has been discovered in the 1950s and have become an important material commercially and technologically nowadays. The most familiar applications of hexaferrites are in magnetic recording and data storage devices. Hexagonal ferrites are referred to the group of M, Y, W, Z, X and U-ferrites. Out of these six hexaferrites, Y type hexaferrites has become much widespread in both research as well as in technological application due to its marvellous dielectric and magnetic behaviour[7]. So, for the present study, Y type hexaferrites is chosen as a research topic. To improve the electrical, structural and magnetic properties of Y-type hexagonal nano ferrites studies has been done using dopant Zn, Cu, Co, Al, Cr [8-10]. But no such study is available with dopant bismuth and cobalt for y type hexaferrite. So, for present research has been taken into consideration for the study of structural and magnetic properties of Bi and Co doped Y type hexaferrites [11, 12].

2. Synthesis Method:

Equal stoichiometry of AR Grade metal nitrates is dissolved in distilled water in clean beaker. The required amount of ammonia is added to the solution so as to maintain pH =7. With the help of magnetic stirring, solution is stirred together till the homogeneous gel is

formed. Once the homogeneous gel is formed it is then taken for heating over a hot plate at around 400 °C for 4 hours. Required Sample in powder form will be formed. Auto combustion of sample is done in a Furnace at 500°C followed by 900°C for 2 hours and 4 hours respectively. Lastly, it is calcined at 1200°C for 5 hours in Furnace.

3.Characterization Technique

3.1 XRD Analysis

XRD of the sample $Sr_2Co_{2-x}Bi_xFe_{12}O_{22}$ (x=0.0 and 0.05) is shown here. The XRD patterns reveal the formation of Y-type hexaferrite [6]. To find the lattice parameters and cell volume (V) following formulas (Equation 1-3) were used:

(1)

(2)

$$D = \frac{k\lambda}{\beta \cos\theta} \quad (3)$$

The various lattice parameters have been given in Table 3.1. With the increase in doping the intensity of the peaks increased. This can be attributed due to the more ionic size of Bi ion (103pm) than Fe ion (60pm). The Bi ion substituted of at tetrahedral sites has pushed the Fe ions into the octahedral sites. However, Particle size first decreases and then increases with Bi doping concentration. No correlation between increase in cell volume and crystal size with increase in Bi content has been found as shown in **Figure 3.1.**

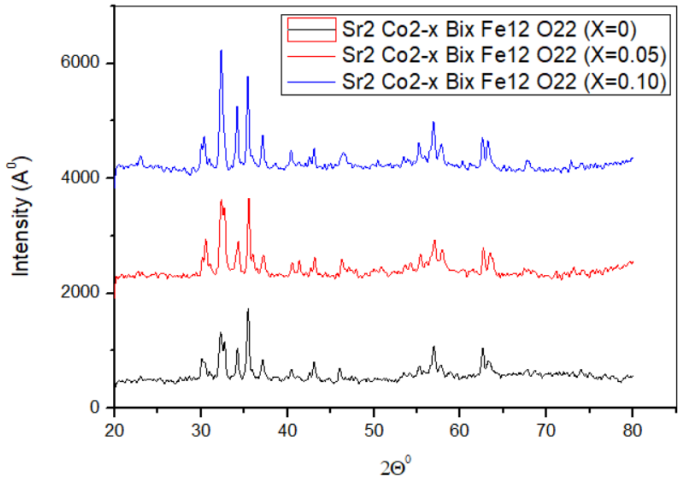

Fig 3.1: XRD Patterns of hexaferrite $Sr_2Co_{2-x}Bi_xFe_{12}O_{22}$ (x=0.0,0.05 and x=0.10)

Table 3.1: Value of lattice parameters calculated for Y type hexaferrite

Sample (x)	Lattice constant a (Å)	Lattice constant c (Å)	Cell Volume (Å)	c/a	D(nm)
0	5.86	43.632	1298.43	7.44	0.29
0.05	5.89	43.3644	1304.02	7.36	0.15
0.10	5.88	43.00	1239.65	7.31	0.28

3.2 FTIR Analysis

Fourier Transform Infrared Spectroscopy is a best method which gives adequate information about the structure of the compound. This technique measures how much of infrared radiation is absorbed by the material with respect to wavelength. It helps us find out the Chemical and structural changes that may occur in the sample when it undergoes combustion and sintering. The wavelengths which are absorbed by the sample reveal the molecular characteristics of the structure. The two-absorption band has been found between 400- 600 cm^{-1} indicates the twisting of Fe-O bond (figure 3.2). The band obtained near to 400- 500 cm^{-1} indicates twisting of Fe-O bond at octahedral sites and band near 550-590cm^{-1} indicates broadening of Fe-O bond at tetrahedral sites.

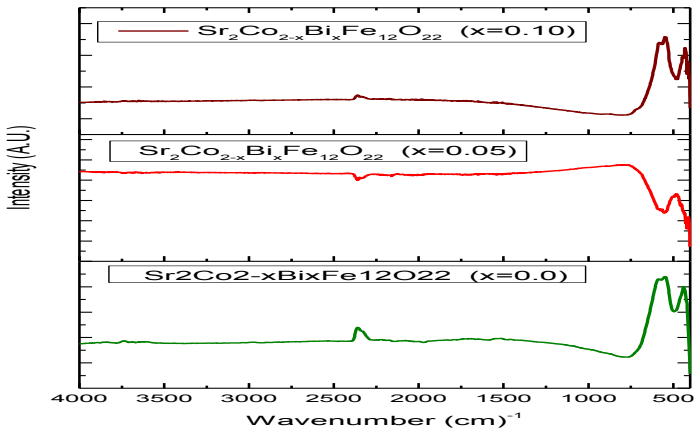

Figure 3.2 FTIR spectra of $Sr_2CO_{2-X}Bi_xFe_{12}O_{22}$ (x=0.0, 0.05, 0.10))

3.3 Magnetic Study:

The hysteresis loop obtained from VSM study $Sr_2CO_{2-X}Bi_xFe_{12}O_{22}$ (x=0.0, 0.05, 0.10)) were plotted in **Figure 3.3**. The significant decrease in M_s Values, while reverse in M_r and Hc values with dopants concentration has been found (**Table 3.2)**. This might be due to magnetic moment of dopants (0.26μB for Bi) which is less than that of iron (Fe^{3+} =5μB). These studies further indicate that magnetic properties are related with dopants ion distribution at various sites and also on vacant sites (act as pinning centers of domain walls) created by dopants ion at the position of Fe^{3+}. The squareness ratio (M_r/ M_s) of less than 0.5 for all compositions reveals that nanoparticles are haphazardly oriented multi domain particles. The coercivity increases with increase in Bi ion concentration while saturation magnetization decreases. There is net increase in magnetic moment of the samples which might be owe to relocation of cations at interstitial sites A and B [13, 14-18].

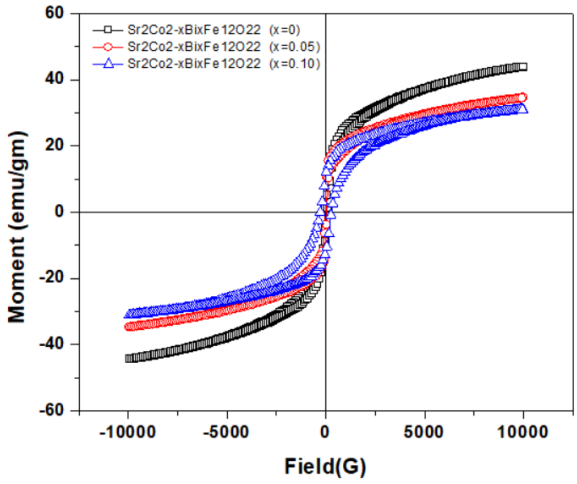

Figure 3.3 The M-H hysteresis loop of $Sr_2CO_{2-X}Bi_xFe_{12}O_{22}$ (x=0.0, 0.05, 0.10))

Table3.2: Magnetic parameters of $Sr_2CO_{2-X}Bi_xFe_{12}O_{22}$ (x=0.0, 0.05, 0.10))

Sr_2 Co_{2-x} Bi_x Fe_{12} O_{22}	Ms (emu/g)	Mr (emu/g)	Hc (Oe)	SR (Mr/Ms)	K (HA^2/kg)	μ_B
x=0	39.2	3.135	30.07	0.07	0.004713484	3.48
x=0.05	34.65	6.94	41.18	0.20	0.014289493	7.72
x=0.10	31	10.85	276.61	0.35	0.150061276	12.09

4 Conclusion:

The Y-type hexaferrite samples are prepared using the sol gel combustion method. In order to reveal the structural properties XRD and FTIR has been done. The magnetic properties indicate that as Bi ion concentration increases, squareness ratio, coercivity and hence net magnetic moment increases which make it best suitable material for magnetic applications.

References:

1) Smit J, Wijn H P J 1959, Ferrites (Philips' Technical Library, Eindhoven,1959)
2) Shen S, Chai Y, Sun Y 2015, Scientific Reports 5 8254.
3) Mukherjee, R., Lawes, G., & Nadgorny, B. (2014). Enhancement of high dielectric permittivity in CaCu3Ti4O12/RuO2 composites in the vicinity of the percolation threshold. Applied Physics Letters, *105*(7), 072901.
4) Mukherjee, R. (2020). Electrical, thermal and elastic properties of methylammonium lead bromide single crystal. Bulletin of Materials Science, *43*(1), 1-5.
5) Mahmood S. H., Jaradat, F. S., Lehlooh, a.-F. & Hammoudeh, a. (2014) Structural properties and hyperfine interactions in Co–Zn Y-type hexaferrites prepared by sol–gel method. Ceram. Int. 40, 5231–5236
4) Nakamura, S., Tsunoda, Y. & Fuwa, A. (2012) Mössbauer study on Y-type hexaferrite Ba 2 Mg 2 Fe 12 O 22. 49–52 doi:10.1007/s10751-011-0486-2
5) Kumar S, Singh V, Aggarwal S, Mandal UK, and Kotnala R K (2010) Synthesis of nanocrystalline Ni0.5Zn0.5Fe2O4 ferrite and study of its magnetic behavior at different temperatures.Materials Science and Engineering B 166:76–82.
6) Basandrai D, Bedi RK, Dhami A, Sharma J, Narang SB, Pubby K, Srivastava AK (2017) Radiation Losses in the Microwave X Band in Al-Cr Substituted Y-Type Hexaferrites Chin. Phys. Lett. 34: 4
7) Basandrai, D., Bedi, R. K., Dhami, A., Sharma, J., Bindra, S., Pubby, K., and Srivastava, A., (2018) Aluminum and Chromium substituted Z-type hexaferrites for antenna and microwave absorber applications Journal of Sol-Gel Science and Technology., 85(1), 59-65
8) S Shah, OP Pandey, J Mohammed, AK Srivastava, A Gupta, **D Basandrai** (2020) Reduced graphene oxide (RGO) induced modification of optical and magnetic properties of M-type nickel doped barium hexaferrite Journal of Sol-Gel Science and Technology DOI 10.1007/s10971-019-05210-0

9) Mukherjee, R., Huang, Z. F., & Nadgorny, B. (2014). Multiple percolation tunneling staircase in metal-semiconductor nanoparticle composites. Applied Physics Letters, *105*(17), 173104.

10) Laha, S. S., Mukherjee, R., & Lawes, G. (2014). Interactions and magnetic relaxation in boron doped Mn3O4 nanoparticles. *Materials Research Express*, *1*(2), 025032.

11) Ansari, K. R., Quraishi, M. A., Singh, A., Ramkumar, S., & Obote, I. B. (2016). Corrosion inhibition of N80 steel in 15% HCl by pyrazolone derivatives: electrochemical, surface and quantum chemical studies. *RSC advances*, *6*(29), 24130-24141.

12) Mukherjee, R., Chuang, H. J., Koehler, M. R., Combs, N., Patchen, A., Zhou, Z. X., & Mandrus, D. (2017). Substitutional Electron and Hole Doping of WSe 2: Synthesis, Electrical Characterization, and Observation of Band-to-Band Tunneling. Physical Review Applied, *7*(3), 034011.

13) Trukhanov, S. V., Trukhanov, A. V., Salem, M. M., Trukhanova, E. L., Panina, L. V., Kostishyn, V. G., ... & Sivakov, V. (2018). Preparation and investigation of structure, magnetic and dielectric properties of (BaFe11. 9Al0. 1O19) 1-x-(BaTiO3) x bicomponent ceramics. *Ceramics International*, *44*(17), 21295-21302.

14) Mohammed, J., Hafeez, H. Y., Adamu, B. I., Wudil, Y. S., Takai, Z. I., Godara, S. K., & Srivastava, A. K. (2019). Tuning the dielectric and optical properties of PrCo–substituted calcium copper titanate for electronics applications. *Journal of Physics and Chemistry of Solids*, *126*, 85-92.

[15] Kumar, P., Khatri, T., Bawa, H., & Kaur, J. (2017, July). ZnO-Fe2O3 heterojunction for photocatalytic degradation of victoria blue dye. In *AIP Conference Proceedings* (Vol. 1860, No. 1, p. 020065). AIP Publishing LLC.

[16] KUMAR, P., SAMIKSHA, S., & GILL, R. (2018). Carbon Monoxide Gas Sensor Based on Fe-ZnO Thin Film. *Asian Journal of Chemistry*, *30*(12), 2737-2742.

[17] Thakur, A., Kumar, A., Kumar, P., Nguyen, V. H., Vo, D. V. N., Singh, H., ... & Kumar, D. (2020). Novel synthesis of advanced Cu capped Cu2O nanoparticles and their photo-catalytic activity for mineralization of aqueous dye molecules. *Materials Letters*, *276*, 128294.

[18] Gill, R., Ghosh, S., Sharma, A., Kumar, D., Nguyen, V. H., Vo, D. V. N., ... & Kumar, P. (2020). Vertically aligned ZnO nanorods for photoelectrochemical water splitting application. *Materials Letters*, *277*, 128295.